JOURNAL OF SOLID STATE CHEMISTRY 95, 307–312 (1991)

Luminescence of Gd^{3+} Activated $LiNaY_2F_8$

A. AAMILI, R. MAHIOU,[1] C. LINARES,* D. ZAMBON,
D. AVIGNANT, AND J. C. COUSSEINS

*Laboratoire de Chimie des Solides, URA 444, CNRS, Université Blaise Pascal et ENSCCF, F-63177 Aubière Cedex, France; and *Laboratoire de Physico-Chimie des Matériaux Luminescents, URA 442 CNRS, Université Claude Bernard, Lyon I, F-69622 Villeurbanne Cedex, France*

Received March 14, 1991

The luminescence of Gd^{3+} in $LiNaY_2F_8$ is reported. The confirmation of the crystal structure is deduced from the emission and excitation spectra recorded at room temperature. It is shown that the Gd^{3+} ions are randomly distributed over the two sites of the Y^{3+} ions. Sets of crystal field parameters are proposed and the various lines are assigned to each site.

Introduction

Optical absorption and fluorescence spectra of lanthanides with $4f^n$ electronic configurations in the solid state are as characteristic of the nature and the structure of the compound as the X-ray powder patterns. As a matter of fact, each chemical compound exhibits an absorption or emission spectrum, whatever its complexity, which is unique and characteristic. This is due to the combination of the effects on the $4f^n$ atom of both structural characteristics and parameters related to the chemical bond such as geometry, bond angles, and lanthanide–ligand distance.

The ground state of the $4f^7$ configuration of the Gd^{3+} ion is $^8S_{7/2}$; this level is only slightly split by the crystal field, therefore it is possible to deduce some information concerning the multiplicity of the regular sites from the number of components of the $^6P_J \leftrightarrow {}^8S_{7/2}$ transitions ($J = 7/2, 5/2, 3/2$). Moreover, the ^6P_J manifolds are perfectly separated from each other. Therefore, it is not necessary to cool the samples to the very low temperatures to reach the position of the first excited ^6P_J levels.

Thus the relative simplicity of the Gd^{3+} optical spectra is utilized to answer structural problems or to give further information (*1–6*).

We report here the results of our investigation on the luminescence of $LiNaY_2F_8 : Gd^{3+}$ and discuss them in relation to the structural data.

Experimental

All luminescence measurements were performed on polycrystalline samples. The $LiNaY_{2-x}Gd_xF_8$ compounds are synthesized in the solid state by reacting stoichiometric mixtures of the starting fluorides: LiF

---

[1] To whom correspondence should be addressed.

0022-4596/91 $3.00

(Merck: 99.98%), NaF (Prolabo: 99.9%), YF_3, and GdF_3 (prepared from Y_2O_3 and Gd_2O_3, Rhône-Poulenc: 99.9%). The mixtures, finely ground, were introduced in sealed nickel tubes and heated at 680°C, for 16 hr. This reaction was immediately followed by an efficient water quenching. The compounds are pure white. Four samples were prepared in this way for the following x values: 0.1, 0.2, 0.3, and 0.4 (molecular concentration $C\% = 50x$).

The X-ray powder patterns obtained on our samples clearly showed that the host $LiNaY_2F_8$ matrix could not accommodate more than 20% Gd^{3+} ion without deformation. For $x > 0.4$ a two-phase region was observed.

The experimental device used for the optical measurements has been previously described (*4*). (resolutions: Emission 0.02 nm; Excitation 0.005 nm).

Structural Background

$LiNaY_2F_8$ fluoride crystallizes in the monoclinic system, with the space group $P2_1/m$ (*7*). The unit cell contains two formula units. In this structure, there are two crystallographically independent yttrium atoms, each occupying a $2e$ site (point symmetry C_s).

A. Dib *et al.* (*8*) carried out a structural determination of the homologous LiNa Yb_2F_8 phase, which has been described in the monoclinic system with $C2/c$ space group. In this structure, the Yb^{3+} ions occupy a single $8e$ site, with point symmetry C_1.

A crystal chemical study (*9*) of the homologous $LiNaLn_2F_8$ (Ln = Ho → Lu) phases has shown that all their X-ray powder patterns could be indexed on the basis of a monoclinic cell corresponding to the $P2_1/m$ space group; an ambiguity concerning the choice of the unit cell subsisted. Besides, the fluorescence spectra of $LiNaY_2F_8 : Eu^{3+}$ (*10*) do not give any evidence for two sites occupied by the Eu^{3+} ion substituting for the Y^{3+} ion. For this reason we decided to use the Gd^{3+} local structural probe in order to clarify this structural problem.

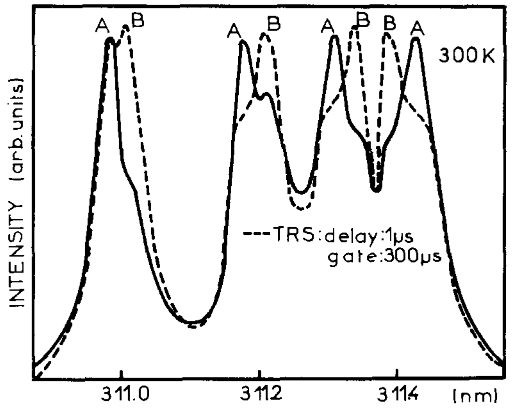

FIG. 1. $^6P_{7/2} \rightarrow {}^8S_{7/2}$ emission spectra of $LiNaY_{1.8}Gd_{0.2}F_8$ at 300 K; — integrated spectrum, --- time resolved spectrum (delay: 1 μs; gate width: 300 μs).

Results

Luminescence Emission and Excitation

The spectra, shown in Figs. 1 and 2, were recorded at 300 K upon excitation at 311 nm ($^8S_{7/2} \rightarrow {}^6P_{7/2}$ transition). The emission lines

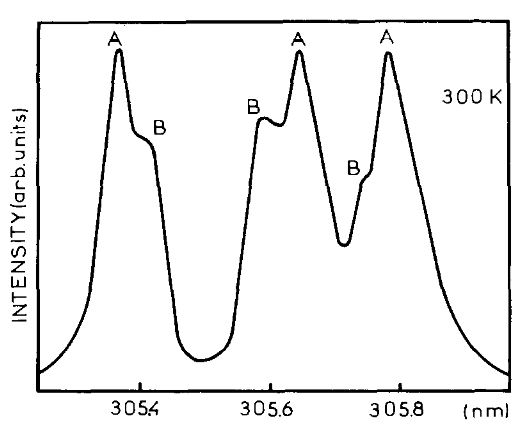

FIG. 2. $^6P_{5/2} \rightarrow {}^8S_{7/2}$ emission spectrum of $LiNaY_{1.8}Gd_{0.2}F_8$ at 300 K.

correspond to the radiative relaxation from the ${}^6P_{7/2}$ and ${}^6P_{5/2}$ Stark levels to the ${}^8S_{7/2}$ ground state. We found eight separate lines for the ${}^6P_{7/2} \rightarrow {}^8S_{7/2}$ transition and six lines for the ${}^6P_{5/2} \rightarrow {}^8S_{7/2}$ transition. The line profiles are independent of the wavelength and of the power of the excitation beam. These results imply that the Gd^{3+} ions present in the structure are divided into two crystallographically independent sites.

In Figs. 1 and 2, the peaks related to the two Gd^{3+} sites are respectively designated as A and B. This differentiation is clearly marked on the emission spectrum of the ${}^6P_{7/2} \rightarrow {}^8S_{7/2}$ transition resolved a short time after the laser pulse (Fig. 1), where it can be seen that the B lines become the more intense ones.

In the case of the Gd^{3+} or Eu^{3+} activated $LiNaYb_2F_8$ compounds, the ${}^6P_{7/2} \rightarrow {}^8S_{7/2}$ and ${}^5D_0 \rightarrow {}^7F_0$ emission spectra recorded between 300 and 77 K show symmetric but broadened lines. This broadening is attributed to the fact that the ionic radii of the Gd^{3+} or Eu^{3+} ions are greater than that of the Yb^{3+} ion. This observation agrees with the uniqueness of the site occupied by the rare earth ion substituting for the ytterbium ion.

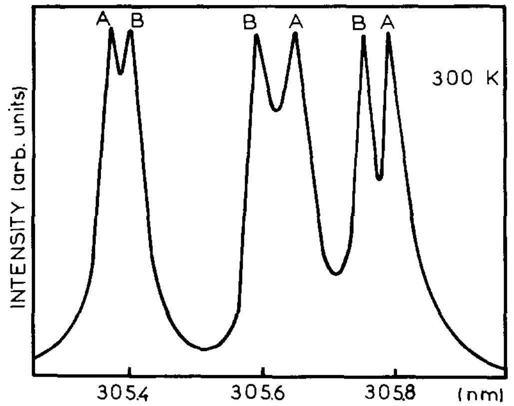

FIG. 4. ${}^8S_{7/2} \rightarrow {}^6P_{5/2}$ excitation spectrum at 300 K.

The excitation spectra of the ${}^6P_{7/2} \rightarrow {}^8S_{7/2}$ luminescence has been recorded at room temperature, scanning the laser wavelengths around the ${}^6P_J$ manifolds ($J = 7/2$, $5/2$, $3/2$). Figures 3, 4, and 5 show the spectra obtained for $LiNaY_{1.8}Gd_{0.2}F_8$. These spectra are independent of the A or B monitored lines. The experimental wavelength and transition energy values are given in Table I. It can be seen that the ${}^8S_{7/2} \rightarrow {}^6P_{3/2}$ absorption transition exhibits only two peaks. For this transition, the excitation lines related to the two sites are overlapped.

Moreover, as the Gd^{3+} ion concentration is increased, the energy of the barycenter of

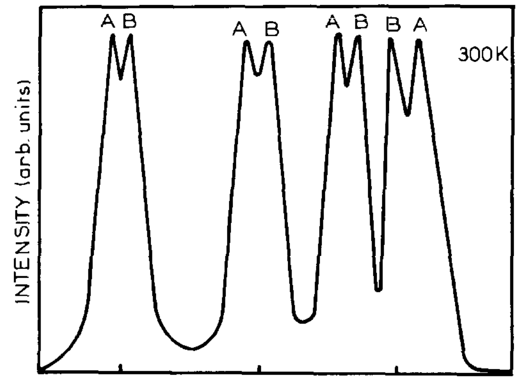

FIG. 3. ${}^8S_{7/2} \rightarrow {}^6P_{7/2}$ excitation spectrum at 300 K.

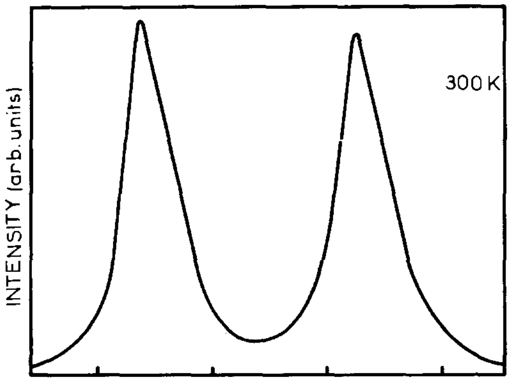

FIG. 5. ${}^8S_{7/2} \rightarrow {}^6P_{3/2}$ excitation spectrum at 300 K.

TABLE I

OBSERVED AND CALCULATED POSITIONS AND ASSIGNMENTS OF THE $^8S_{7/2} \rightarrow {}^6P_J$ EXCITATION LINES OF Gd^{3+} IN $LiNaY_2F_8$

Nominal state	Experimental energies in cm^{-1} (wavelengths in nm)	Barycenter in cm^{-1} (wavelengths in nm)	Calculated energies in cm^{-1} (wavelengths in nm)		
			Set 1	Set 2	Set 3
			Site A		
$^6P_{3/2}$	33,317.8 (300.14)	33,307.6	33,317.5 (300.14)	33,317.4 (300.14)	33,317.2 (300.15)
	33,297.3 (300.32)	(300.23)	33,297.7 (300.32)	33,297.8 (300.32)	33,298.0 (300.32)
	32,747.2 (305.37)		32,738.4 (305.45)	32,738.7 (305.45)	32,738.4 (305.45)
$^6P_{5/2}$	32,727.2 (305.65)	32,722.2	32,720.7 (305.62)	32,719.7 (305.63)	32,719.9 (305.62)
	32,702.2 (305.79)	(305.60)	32,707.5 (305.74)	32,708.2 (305.73)	32,708.3 (305.73)
	32,155.4 (310.99)		32,162.7 (310.92)	32,163.0 (310.92)	32,162.3 (310.92)
$^6P_{7/2}$	32,134.7 (311.19)	32,130.6	32,137.8 (311.16)	32,137.6 (311.16)	32,137.8 (311.16)
	32,122.3 (311.31)	(311.23)	32,119.8 (311.33)	32,117.3 (311.36)	32,117.7 (311.35)
	32,109.9 (311.43)		32,102.1 (311.51)	32,104.5 (311.48)	32,104.6 (311.48)
			Site B		
$^6P_{3/2}$	33,317.8 (300.14)	33,307.6	33,316.0 (300.16)	33,315.9 (300.16)	33,316.0 (300.16)
	33,297.3 (300.32)	(300.23)	33,299.2 (300.31)	33,299.3 (300.31)	33,299.2 (300.31)
	32,743.9 (305.40)		32,738.8 (305.45)	32,738.6 (305.45)	32,739.0 (305.45)
$^6P_{5/2}$	32,723.6 (305.59)	32,724.7	32,722.6 (305.60)	32,722.8 (305.60)	32,722.2 (305.60)
	32,706.5 (305.75)	(305.58)	32,712.7 (305.69)	32,712.7 (305.69)	32,712.9 (305.69)
	32,153.3 (311.01)		32,158.0 (310.96)	32,157.0 (310.97)	32,157.9 (310.97)
$^6P_{7/2}$	32,132.6 (311.21)	32,129.8	32,134.6 (311.19)	32,135.8 (311.18)	32,135.8 (311.18)
	32,119.2 (311.34)	(311.24)	32,118.9 (311.34)	32,119.0 (311.34)	32,117.4 (311.36)
	32,114.1 (311.39)		32,107.7 (311.45)	32,107.7 (311.45)	32,108.1 (311.45)

the ^6P_J Stark components relative to each site raises the higher energies; at the same time, the splitting of the levels decreases. This nephelauxetic effect and the resulting crystal field variation are attributed to the fact that the Gd^{3+} ionic radius is greater than that of Y^{3+} (*5, 11*).

Crystal Field Parameters

It is well known that the splittings of the ^6P_J levels (J = 7/2, 5/2, 3/2) for Gd^{3+} depend exclusively on second-order crystal field parameters (*11, 12*). By neglecting J-mixing, we can obtain the value of these parameters by using Stevens' equivalent operators (*13, 14*). Using Wybourne's notation (*15*), the three independent sets of B_0^2 and B_2^2 crystal field parameters given in Table II are those which lead to the best agreement between the experimental and calculated ^6P_J (J = 7/2, 5/2, 3/2) energy levels which are reported in Table I.

The average quadratic error for the nine ^6P levels for both A and B sites are, respectively, the following:

5.2 cm^{-1} and 3.9 cm^{-1} for the first set.
5.1 cm^{-1} and 3.9 cm^{-1} for the second set.
5.1 cm^{-1} and 4.0 cm^{-1} for the third set.

These errors do not allow us to select one of the three parameter series. A similar calculation on the $^5D_0 \rightarrow {}^7F_1$ transition of Eu^{3+} in $LiNaY_{1.9}Eu_{0.1}F_8$ (Stark components at 16,955, 16,878, and 16,852 cm^{-1} at 77 K (*10*)) leads to the three parameter sets given in Table III. Let us remember that using the Eu^{3+} ion as dopant, it cannot be distin-

TABLE II

CRYSTAL FIELD PARAMETERS FOR Gd^{3+} IN $LiNaY_2F_8$

	Set 1		Set 2		Set 3	
Site	B_0^2(cm^{-1})	B_2^2(cm^{-1})	B_0^2(cm^{-1})	B_2^2(cm^{-1})	B_0^2(cm^{-1})	B_2^2(cm^{-1})
A	−270	±82	+80	±196	+200	±143
B	−240	±41	+60	±167	+160	±135

guished between both Y^{3+} sites from the fluorescence spectra analysis.

These parameters are very close to those found for Gd^{3+}. It is difficult to choose between these three parameter sets. This ambiguity can be removed by analysing the polarization of the $^5D_0 \rightarrow {}^7F_1$ emission of the Eu^{3+} ion on a single crystal.

Relation with the Crystal Structure

It can be noted that the crystal field parameters (Table II) are very close for the two sites. At the same time, their values are smaller for the B site, the splitting being weaker. It is well known that the splitting decreases as the distance to the ligand increases (*16*). By referring to the crystal structure of $LiNaY_2F_8$ (*7*), one finds that the Y–F distances are close. On the other hand, they are slightly weaker for the yttrium atoms noted Y(1) in Table IV (average distance Y(1)–F: 2.2584 Å and average distance Y(2)–F: 2.2595 Å). This is also valid for the Gd–F distances in $LiNaY_2F_8$: Gd^{3+}. Therefore, it is possible to assign the A lines to the Gd^{3+} ions on the Y(1) site and the B lines to the Gd^{3+} ions on the Y(2) site.

Discussion

The results obtained indicate that for the Y^{3+} or Gd^{3+} ions in $LiNaY_2F_8$, two sites with the same coordination and point symmetry are characterized by the Gd^{3+} fluorescence spectra, showing in this way the small variations of bond angles and distances. It is moreover interesting to note the very weak difference between the barycenters of the levels relative to the A and B sites (<3 cm^{-1} for the ^6P_J terms, whatever the gadolinium concentration in the investigated series may be). This information implies that the nephelauxetic shift for the two sites are equivalent. Thus, the Gd–F (or Y–F) distances in each of the two sites are very close, in agreement with the crystallographic data.

Consequently, the Gd^{3+} ion is a structural site probe which is especially sensitive regarding the coordination polyhedra.

TABLE III

CRYSTAL FIELD PARAMETERS FOR Eu^{3+} IN $LiNaY_2F_8$

	Set 1	Set 2	Set 3
B_0^2(cm^{-1})	−300	+85	+215
B_2^2(cm^{-1})	±53	±210	±157

TABLE IV

DIFFERENT Y–F DISTANCES IN $LiNaY_2F_8$

Y(1)–F distances (Å)		Y(2)–F distances (Å)	
Y(1)–F(4)	2.183 (14)	Y(2)–F(3)	2.185 (6)
Y(1)–F(3)	2.192 (6)	Y(2)–F(4)	2.200 (33)
Y(1)–F(2)	2.205 (8)	Y(2)–F(2)	2.201 (8)
Y(1)–F(6) (×2)	2.228 (4)	Y(2)–F(5) (×2)	2.228 (4)
Y(1)–F(6) (×2)	2.310 (5)	Y(2)–F(5) (×2)	2.308 (5)
Y(1)–F(1)	2.411 (6)	Y(2)–F(1)	2.418 (6)

In conclusion, all experimental observations confirm the structural description given in the $P2_1/m$ space group by D. Avignant *et al.* (*7*) during the structural study of the $LiNaY_2F_8$ compound.

References

1. C. Guttel, E. Antic, and P. Caro, *Phys. Status Solidi B* **81,** 463 (1977).
2. W. Jeitschko, *Acta Crystallogr., Sect. B* **28,** 60 (1972).
3. J. Fava, Nguyen-trut-Dinh, and G. Le Flem, *Mater. Res. Bull.* **14,** 683 (1979).
4. R. Mahiou, A. Arbus, J. C. Cousseins, and M. T. Fournier, *J. Less-Common Met.* **136,** (1), 9 (1987).
5. R. Mahiou, J. Metin, M. T. Fournier, and J. C. Cousseins, *Mater. Res. Bull.* **23,** 1389 (1988).
6. R. Mahiou, J. C. Cousseins, and M. T. Fournier, *J. Chim. Phys.* **85,** 769 (1988).
7. D. Avignant, D. Zambon, J. Metin, and J. C. Cousseins, *Rev. Chim. Miner.* **21,** 771 (1984).
8. A. Dib, M. F. Gorius, and S. Aleonard, *J. Solid State Chem.* **65,** 205 (1986).
9. D. Zambon, J. Metin, B. Picaud, and D. Avignant, *C.R. Acad. Sci. Paris Ser. 2* **301**(17), 1235 (1985).
10. D. Zambon, J. Metin, J. C. Cousseins, and M. T. Fournier, *J. Less-Common Met.* **143,** 345 (1988).
11. E. Antic-Fidancev, M. Lemaître-Blaise, and P. Caro, *J. Chem. Phys.* **76,** 2906 (1982).
12. H. D. Jones and B. R. Judd, *Phys. Rev. B* **2,** 2319 (1970).
13. K. W. H. Stevens, *Proc. Phys. Soc. London, Sect. A* **65,** 209 (1952).
14. G. H. Dieke, "Spectra and Energy Levels of Rare Earths Ions in Crystals," Interscience, New York (1968).
15. B. G. Wybourne, "Spectroscopic Properties of Rare Earths Ions in Crystals," Interscience, New York (1968).
16. P. Caro, E. Antic, L. Beaury, O. Beaury, J. Derouet, M. Faucher, C. Guttel, O. K. Moune, and P. Porcher, "Colloque International du CNRS–Lyon (1976)," p. 71, Editions du CNRS, Paris, (1977).